COARSENING IN SOLID-LIQUID MIXTURES: OVERVIEW OF EXPERIMENTS ON SHUTTLE AND ISS

W.M. B. Duval[1], R.W. Hawersaat[1] , T. Lorik[2], J. Thompson[3], B. Gulsoy[3], P.W. Voorhees[3]

[1]NASA Glenn Research Center, Cleveland, Ohio 44135
[2]Zin Technologies, Cleveland, Ohio 44130
[3]Northwestern University, Evanston, IL 60208

Keywords: Ostwald ripening, coarsening, kinetics, microgravity

Abstract

The microgravity environment on the Shuttle and the International Space Station (ISS) provides the ideal condition to perform experiments on Coarsening in Solid-Liquid Mixtures (CSLM) as deleterious effects such as particle sedimentation and buoyancy-induced convection are suppressed. For an ideal system such as Lead-Tin in which all the thermophysical properties are known, the initial condition in microgravity of randomly dispersed particles with local clustering of solid Tin in eutectic liquid Lead-Tin matrix, permitted kinetic studies of competitive particle growth for a range of volume fractions. Verification that the quenching phase of the experiment had negligible effect of the spatial distribution of particles is shown through the computational solution of the dynamical equations of motion, thus insuring quench-free effects from the coarsened microstructure measurements. The low volume fraction experiments conducted on the Shuttle showed agreement with transient Ostwald ripening theory, and the steady-state requirement of LSW theory was not achieved. More recent experiments conducted on ISS with higher volume fractions have achieved steady-state condition and show that the kinetics follows the classical diffusion limited particle coarsening prediction and the measured 3D particle size distribution becomes broader as predicted from theory.

Introduction

The late stage of first-order phase transformation can result in a polydisperse two-phase mixtures composed of a dispersed second phase in a matrix whose evolution is driven by surface energy in a diffusional process known as Ostwald ripening or coarsening. For a binary alloy system such as Lead-Tin (Pb-Sn) with finite volume fractions of Tin, coarsening is driven by capillary-induced concentration gradients which depend on local curvature of spherical particles in the slightly supersaturated matrix. This process can also drive interparticle diffusional interaction between the particles in the matrix depending on the volume fraction. The system is relaxed toward equilibrium by minimizing its energy given by the dependence of its chemical potential on curvature [1, 2]. Minimization of energy in the system occurs through reduction of interfacial area while concomitantly increasing its length scale. The dynamics occur through competitive particle growth, by which the population dynamics evolve through the dissolution of particles smaller than the average particle size and growth of particle larger than the average size through the matrix.

The theory of coarsening has been described by Lifshitz, Slyozov [3] and Wagner [4] (LSW) for an ideal system in which the particles are infinitely separated, no diffusional interaction, which serves as the limit of zero volume fraction. Practical applications of alloy systems require finite volume fractions, thus the LSW limit serves as basis by which coarsening theories for finite volume fractions should converge. Hence performing an experiment by which LSW theory can be tested is quintessential. LSW theory predicts that for the limit of zero volume fraction particles grow with time as the cube root of the average radius, and the particle size distribution becomes independent of time or self-similar at steady-state. However finding a system which satisfies all the constraints of LSW theory is prohibitive for ground-based laboratory condition due to effects of particle sedimentation and buoyancy-induced convection.

The purpose of the experiments on Shuttle and ISS is to permit testing of LSW coarsening theory, by elimination of particle sedimentation and buoyancy-induced convection through the microgravity condition, and to investigate effect of finite volume fractions on coarsening. The measurement of coarsening rate on volume fraction will permit

comparison between various coarsening theories [5-18]. However the coarsening function that describes the volume fraction dependence on the rate constant differs among the different theories. These experiments will help to differentiate predictions from coarsening theories based on statistical mechanics [7-13], effective medium or mean field, [14, 15] and numerical simulation [16-18]. The Lead-Tin system is ideal for such a study because the thermophysical parameters have been measured [19], this permits accurate prediction of the LSW rate constant which is dependent on thermophysical properties only.

Methods

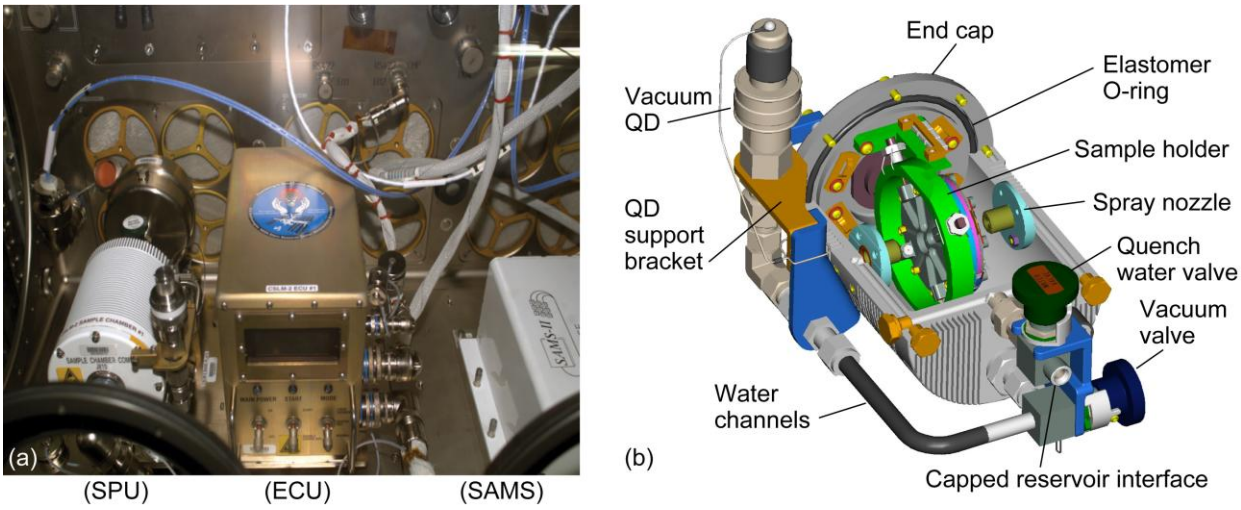

Figure1. Flight hardware installed in the Microgravity Science Glovebox on ISS showing: (a) the sample processing unit (SPU), the electronics control unit (ECU), and the space acceleration measurement system (SAMS); (b) hardware overview of the sample chamber in the SPU.

The flight hardware by which the microgravity experiments were performed is shown in Figure 1 as installed in the Microgravity Science Glovebox (MSG) in the U.S. Laboratory module on ISS. The hardware in Fig. 1a from left to right consists of the sample processing unit (SPU), an electronics control unit (ECU), and the Space Acceleration Measurement System (SAMS) for measuring the local microgravity acceleration. The ECU controls the experiment; the SPU (Fig. 1b) contains the sample holder which houses the heating unit (63.48 mm diameter and 17 mm thick) and the samples for processing, a water reservoir at ambient temperature T = 25 ^{O}C, a pressurized air cylinder to drive quenching, and a vacuum connector used to pump the system to a vacuum level of 0.2 Torr for temperature uniformity in the SPU. The heating system consists of two disc resistance heaters and one ring heater to insure uniform heating with four resistance temperature devices (RTD) installed mid-way between the discs 17.4 mm from the center at an angle of 90^{o} to measure temperature of the samples. Quenching is achieved by forced flow through the spray nozzle (Fig. 1b) driven by air pressure for a duration of 20 sec. The SPU heats material samples up to 185^{o}C in less than 9.5 min, holds the temperature for a predetermined time at 185 ± 0.1 ^{0}C ranging from 0.25 to 48 hrs (coarsening phase), and then quenches the samples to nearly room temperature in approximately 1 minute. The SPU sample holder contains four Lead-Tin samples of 12 mm diameter and 6 mm thickness for various volume fractions of Tin.

In order to produce uniform initial particle size distribution, an acceptable heating sequence to reach the coarsening temperature of 185 ^{o}C has been determined from ground-based experiments as shown in Figure 2a. The melting of the sample from 30 ^{o}C to the thermal arrest slightly above 183 ^{o}C in less than 210 sec is necessary in order to avoid rearrangement of the particle distribution or significant grain growth. The thermal arrest spans a duration of 180 sec followed by the post-melt equilibration period in which the temperature rises to 185 ^{o}C. In order to avoid dissolution of smaller particles, it is necessary to minimize temperature overshoot from the temperature change from the thermal arrest (183 ^{o}C) to the coarsening operating temperature (185 ^{o}C). As temperature isothermality is necessary for the experiment, a temperature gradient less than 1^{o}K/cm is required in order to avoid significant convection which would lead to an inhomogeneous distribution of particles within the sample. These engineering requirements are programmed in the ECU through proportional integral derivative (PID) control of the SPU, coupled with robust design of the heating system to minimize temperature gradient, yield the required temperature isothermality for successful coarsening experiments. The response of RTD2,3,4 to the control RTD1 shows that PID controlled to a fairly tight tolerance (± 0.2 ^{o}C) to approach isothermal conditions.

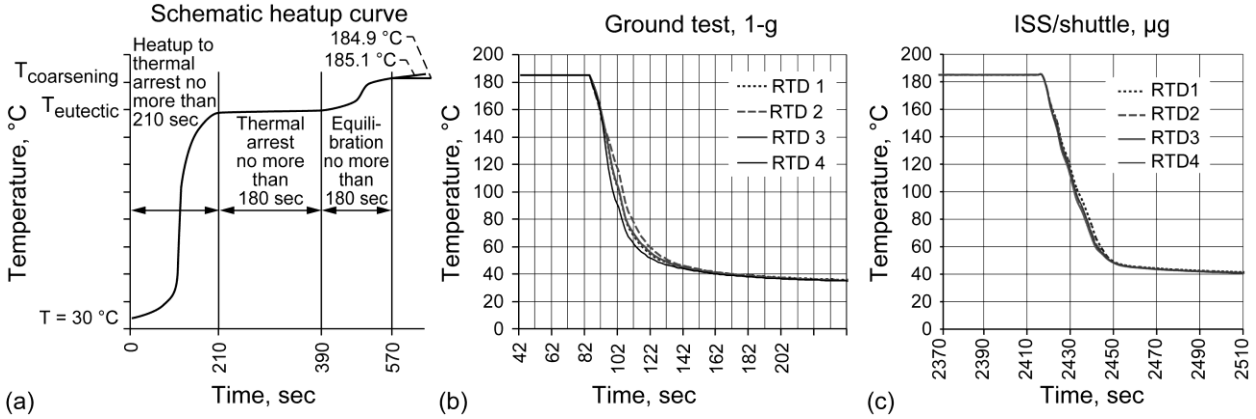

Figure 2. Heating and Quenching profiles for ground-based and microgravity condition showing: (a) heating sequence to reach coarsening temperature, (b) quenching for ground-based condition, and (c) quenching in microgravity.

The effect of quenching is to cause formation of a eutectic solid. This solid is nucleated heterogeneously on the existing solid Tin particles in the liquid; thus, there is very little undercooling below the eutectic temperature. An important parameter that needs to be controlled during the quenching process is the rate of cooling. The cooling rate determines the average spacing of the eutectic solid which forms during the solidification process. A coarse spacing makes it difficult to locate the interface between the particle and the eutectic. Thus, stereological measurements to determine particle size become difficult to perform. From ground-based experiments, it was determined that after the quench is engaged the temperature should drop from 184.9 ^{o}C to 120 ^{o}C in approximately 6 sec and from 120 ^{o}C to 30 ^{o}C in approximately 50 sec. It was also estimated that a temperature gradient less than 100 ^{o}C/cm is required to ensure that particle motion due to a temperature gradient at the solid-liquid interface will not be of concern.

The cooling curves from the SPU shown in Fig. 2b,c represent an acceptable approximation to the cooling requirements, as the microstructure from these cooling curves permitted stereological measurements without major difficulty. It was later determined from a demonstration flight experiment that even slow quench can yield reasonable microstructure, thus the cooling rate can be relaxed. For quenching, RTD1,2,3,4 show response to the cooling boundary condition. Note since the quench is induced by forced jet flow for 20 sec, results from microgravity and ground-based are not significantly different over the time scale of 50 sec for which the temperature has dropped to 50 ^{o}C from the start. However, the flight SPU shows a much longer transient to reach 30 ^{o}C in comparison to ground-based condition due to the reduction of buoyancy-induced convection on Shuttle/ISS.

An issue of concern during quench is the effect of large cooling rate on particles in the liquid matrix over the short time interval prior to solidification. A transient model based on two-dimensional dynamical equations of motion was solved to determine the magnitude of induced velocity as well as particle displacement relative to the average size. The particles in the liquid matrix is approximated as tracer particles, thus the model is most applicable to the low volume fraction range of the experiment. This model implies that the density field is approximated by an equation of state $\rho(T)=\rho(T_a)[1-\beta\triangle T]$; β is the coefficient of thermal expansion (β = 2.14x10^{-5} / ^{o}K), T_a is the coarsening temperature taken as 186 ^{o}C for initial condition, and $\triangle T$ is the driving temperature difference between the sample and the cooling boundary. The sudden cooling introduces a discontinuity of the dynamical equilibrium phase and gives rise to density gradients that are coupled to the temperature field. As a result of coupling of the density field to the body force, a buoyancy flow is generated [20]. The coupled set of incompressible Boussinesq equations (continuity, Navier-Stokes, temperature, and Lagrangian particle motion) are solved using finite-difference techniques with a flux corrected transport algorithm for the nonlinear advective terms of the temperature field [20]. From scaling analysis, it has been shown [21] for an analogous heating problem, that the parametric space for the characteristic velocity magnitude can be given as a function of four parameters,

$$||V|| = ||V||\ (Ra, Ar, Pr, f) \qquad (1)$$

where $Ra = ng_o\beta q_T" D_s^4/k\nu\alpha$, $Ar = D_s/L$, $Pr = \nu/\alpha$, $f = q_{sr}"/q_T"$; $q_T" = q_{sl}" + q_{sr}" + q_{tb}"$

In the above parameters, g_o is the standard gravitational acceleration and n is a ratio which varies depending on the gravitational level (n=1 Earth, n= 10^{-6} Shuttle/ISS), q_T" is the total heat loss at the sample boundary of a disk with subscripts sl, sr, tb, indicating sides left, right and peripheral; D_s and L are sample diameter and thickness, k thermal conductivity, ν the kinematic viscosity, and α the thermal diffusivity in which ($k = 4.09x10^1$ W/m ^oK , $\nu = 2.48x10^{-7}$ m^2/s, $\alpha = 1.033x10^{-5}$ m^2/s). The thermophysical properties needed to estimate the parameters are known for Lead-Tin [22]. For a nominal heat flux condition estimated at $q_{sr}" = 3.49\ x10^3$ W/ m^2, it is assumed that there is equivalent heat loss on all surface boundaries of the cylindrical sample $q_T" = 3q_{sr}"$. This implies that the heat flux ratio (f) which represents the cooling rate is constant, the Prandtl number (Pr) and aspect ratio (Ar) are also constants (f = 0.33, Ar = 2, Pr = 0.024). It can be shown that scaling leads to $||V|| \sim Ra$. This scaling law was verified through numerical simulation shown in Figure 3. The Figure shows that depending on the Rayleigh number, convective level intensity, the flow field can be either conductive or convective. The reference points, evaluated for asymptotic values at t = 10 sec, shown in Fig. 3 for $10^{-6}g_o$ correspond to $Ra = 4.34x10^{-4}$ in which $||V|| = 4.85x10^{-11}$ m/s, T_{min} = 440.3 ^oK, T_{max} = 442.2 ^oK whereas at 1-g_o $Ra = 4.34x10^2$, $||V|| = 4.85x10^{-5}$ m/s and T_{min} = 440.3 ^oK, T_{max} = 442.2 ^oK. In the conductive region, the linearity of the scaling law is verified, $||V|| = U_o Ra$, for $Ra \leq 4.34x10^3$ where $U_o = 1.12x10^{-7}$ m/s. Since U_o is determined from regression, it has the same units as ||V||. Note that the cooling minimum and maximum temperatures (T_{min}, T_{max}) in the sample are equivalent for microgravity and ground-based conditions in agreement with the trends in the cooling curves in Fig. 2b,c. At t = 1 sec T_{min} = 456.2 ^oK and T_{max} = 457.9 ^oK nearly reach the eutectic temperature with $||V|| = 1.88x10^{-11}$ m/s for microgravity which increases by a factor of 10^6 for 1g. The corresponding particle displacement (||r||), for microgravity and ground-based are respectively $||r|| = 4x10^{-4}$ μm and ||r|| = 400 μm. The microgravity particle displacement is much smaller than the average particle size for a typical range of 10 - 70 μm; this implies that quenching does not affect spatial distribution of particles on ISS/Shuttle.

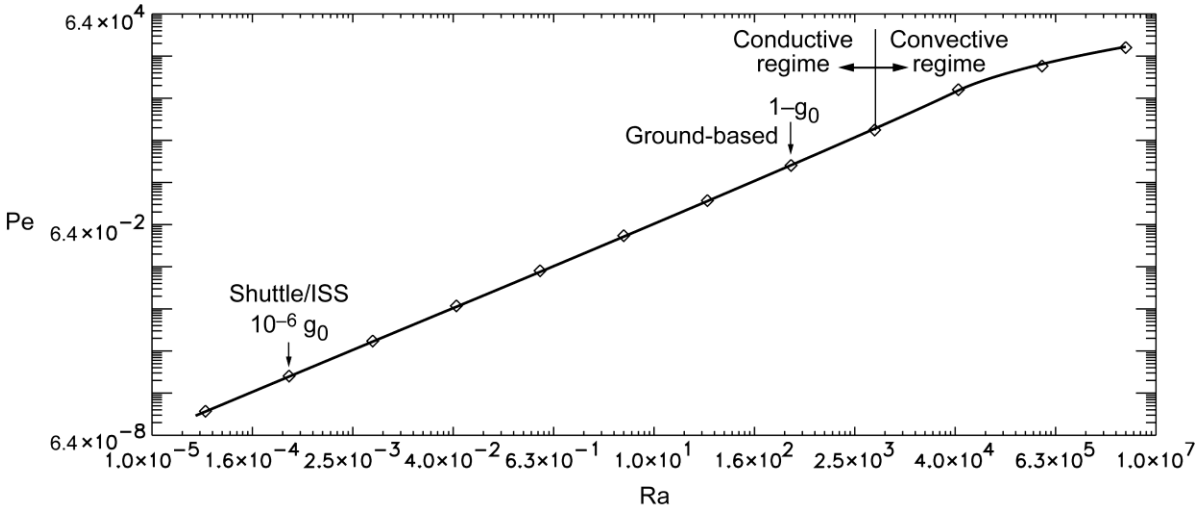

Figure 3. Peclet number (Pe) based on <R> = 40μm as a function of Rayleigh number (Ra) for ground-based and microgravity condition.

An important parameter based on the characteristic velocity ||V|| which characterizes the ratio of mass transport by convection in relation to diffusion is the diffusional Peclet number [23] defined as Pe = ||V|| <R> / D , in which <R> is the average particle radius and D the diffusion coefficient. For small Peclet number, Pe << 1, mass transport is dominated by diffusion which is the required condition for diffusive-coarsening. Figure 3 shows that for microgravity condition Pe <<1 verifying that coarsening occurs by diffusion in microgravity. For the diffusive regime, there is a linear relationship between Pe and Ra given by

$$Pe = U_o <R> Ra / D \qquad (2)$$

where $Pe = 5.5x10^{-6}$ for $10^{-6}g_o$, and Pe = 5.5 for $1g_o$ evaluated for <R> = 70 μm in which $D = 6.26x10^{-10}$ m^2/s [22]. The above analysis shows that the restriction imposed on heating and quenching resulted in diffusion limited particle coarsening for microgravity experiments.

Results and Discussion

The microgravity environment is ideal for the testing of LSW theory, since the experiments have to be performed using finite volume fractions as an approximation to the zero volume fraction limit of the theory. For low volume

fractions, as illustrated in Figure 4, under Earth's gravity sedimentation cause the solid particles to sediment to one side of the specimen (Fig. 4a). In contrast the finding in microgravity (Shuttle/ISS) (Fig. 4b) shows that sedimentation and buoyancy-induced convection effects can be eliminated, thus equi-dispersed particle distribution can be obtained to allow kinetic studies. Given the ideal initial condition, we contrast the low volume fraction results (CSLM-1, Shuttle) 10 % [24, 25] (Fig. 4c) and the findings at higher volume fraction 50% [26] (CSLM-2, ISS) (Fig. 4d). In brief, the low volume fraction experiment show that the particles as they coarsen increase in size with coarsening time while the number of particles decrease; and there is no particle contact as postulated in LSW theory (Fig. 4c). However for higher volume fractions (Fig. 4d) particles are interconnected and deviate from predictions of mean field coarsening theory [14-17] but shows agreement with grain growth theory [26].

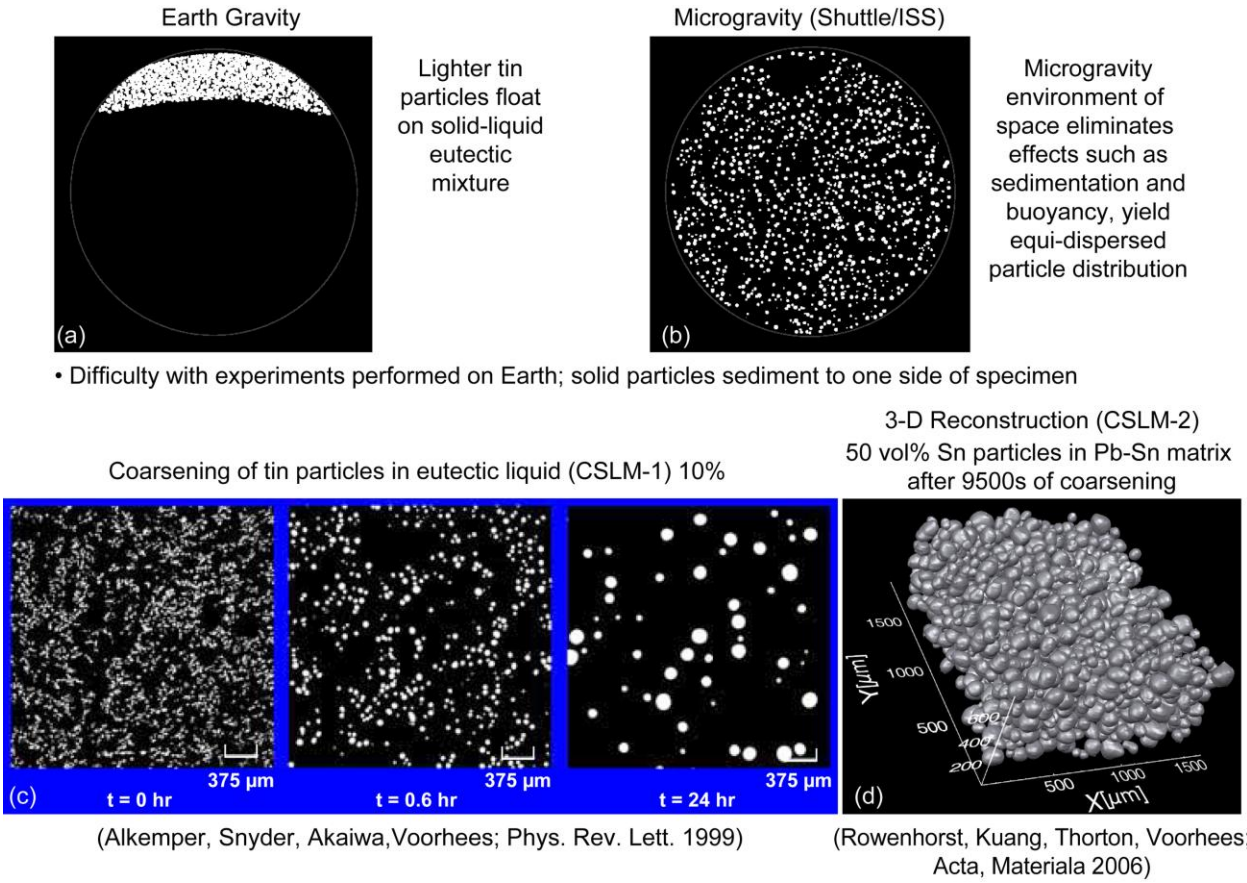

Figure 4. Microstructure of samples contrasting ground-based and microgravity results showing: (a) effect of Earth's gravity, (b) equi-dispersed particle distribution in microgravity, (c) coarsening in microgravity at low 10% volume fraction on Shuttle (CSLM-1), and (d) 3-D reconstruction of 50% volume fraction showing interconnection of particles on ISS (CSLM-2).

The findings for the low volume fraction 10% illustrate the classical description of LSW theory, i.e., the system approaches a steady-state or self-similar regime in which the particle size distribution (PSD), when scaled by the average particle size [24, 25], is time invariant (t = 0.6 hr and t = 24 hr) and is independent of both the initial PSD (t = 0.6 hr) and the parameter of the system (K_{LSW}), for the limit of a vanishing particle volume fraction and in the limit $t \rightarrow \infty$ where t is time. The initial (t = 0) distribution of particles upon melting results in equi-dispersed second phase domains which gives rise to spherical particles at t = 0.6 hr. The kinetics of LSW is dependent on the average particle radius, $\langle R \rangle$ and K_{LSW} by the temporal law,

$$\langle R \rangle^3(t) = \langle R \rangle^3(0) + K_{LSW}\, t \qquad (3)$$

where the LSW rate constant is given by K_{LSW}. The uniqueness of the microgravity experiment is the employment of a system that satisfy all the assumptions employed by theory and in which the thermophysical properties needed to determine K_{LSW} (= 1.1 $\mu m^3/s$) are measured [19] independent of a coarsening experiment. The rate constant is given by, $K_{LSW} = 8\, T_o \Gamma D / 9 M_L (C_S - C_L)$ with M_L the slope of the liquidus curve, and C_S and C_L the compositions of the solid and liquid at a planar solid-liquid interface, T_o the coarsening temperature, Γ the capillary length, and D the

diffusion coefficient. The low volume fraction experiment show that, despite the steady-state assumption of LSW was not realized in this experiment, the temporal growth law kinetics is in agreement with Eq. (1) [24, 25]. The evolution of the spatial correlation function [25] as time increases indicated the presence of transient Ostwald ripening [16, 17] or coarsening. Closure to the above findings can be obtained by performing microgravity experiments in the low volume fraction range in which steady-state is obtained.

The steady-state temporal laws were confirmed for the 30% volume fraction for combined experiments performed on the Shuttle (CSLM-1) and ISS (CSLM-2) shown in Figure 5 [27]. The experiments showed that the coarsening rate on Shuttle and ISS are identical, even though g-jitter on Shuttle is lower than ISS [22]. There was no enhancement of coarsening kinetics due to g-jitter which has been shown using mean field analysis [28]. Analysis of g-jitter effect, using the spectrum from SAMS, on Stokes particle sedimentation [22] showed that g-jitter can cause sedimentation of the large particles which places a maximum bound of 48 hrs for experiments performed on ISS. This finding also indicated that experiments can be done on ISS with volume fraction less than 30% to test LSW theory, since g-jitter was of concern for the low volume fraction coarsening experiments on ISS.

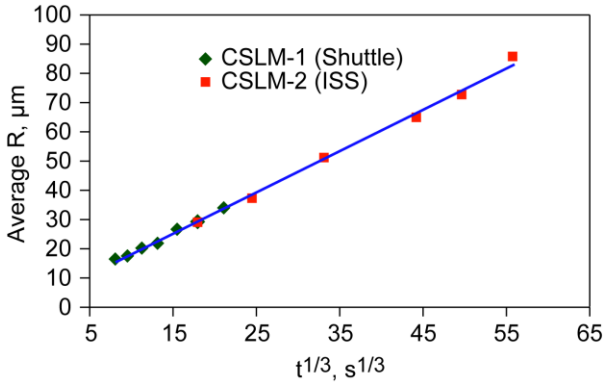

Figure 5. Average particle size for 30% volume fraction contrasting Shuttle (CSLM-1) and ISS (CSLM-2) results, Kammer et al. AIAA 2009-616 [27].

For practical applications with higher volume fractions, there have been several theories [5-18] that remove the restrictive assumption of small volume fraction of the coarsening phase. These theories predict that the cube of the rate constant (K) and shape of the scaled PSD become a function of the volume fraction. In the limit $t \rightarrow \infty$, the exponent of the temporal law is unaltered. The scaled PSD's are predicted to be broader and more symmetric than those given by LSW (Fig. 6b). The rate constant is predicted to vary with volume fraction (Φ) as

$$K(\Phi) = K_{LSW}\, f(\Phi) \qquad (4)$$

where $f(\Phi)$ is the volume fraction dependence of the rate constant and is system independent such that when $\Phi = 0$, $K = K_{LSW}$ (Fig. 6a).

For systems with finite volume fractions of the coarsening phase, the zero volume fraction assumption of LSW in which there is no particle interaction needs to be modified to account for diffusional interaction. The diffusional interactions are included in the theory through a microscopic description of the coarsening process which depends on interparticle separation distance [23]. This description is based on point source/sink approximation to represent emission or adsorption of solute from shrinking or growing particles as input into the Laplacian concentration field. The coupling of the solutal field, for a population of spherical particles, with the restriction placed on mass conservation (rate of change of volume fraction is zero) and the Gibbs-Thompson boundary condition for mass balance at the particle-matrix interface yield a multipole expansion equation that can be used to predict growth rate. However, the properties of importance for experiments are statistically averaged quantities. The statistical average quantities obtained from averaging the microscopic equations fall into three different approaches which includes, effective medium or mean field [14,15,18], statistical mechanics [7-12], and direct numerical simulation [16-18], are shown in Fig. 6a.

The effects of interparticle interactions, in the low volume fraction limit, can be described from first-principles by using the first term in a multipole expansion for the diffusion field in the matrix [23]. This approach, for the monopole expansion, allows the account of diffusional interactions under the assumption that the volume fraction of the coarsening phase is less than approximately 0.1. The numerical simulations are illustrated in Fig. 6a for the

predictions of Beenaker [8], Enomoto, Kawasaki, and Tokuyama (EKT) [7] and Yao, Elder, Guo and Grant (Yao) [18]). Aikawa and Voorhees (AV) [16] have extended the monopole approach to volume fraction of 0.3 by adding dipolar terms to the description of the diffusion field. Relative to the monopole (M) approximation, the addition of a dipolar (M+D) term in Fig. 6a for AV (present M and M+D) is to increase the coarsening rate in comparison EKT.

The effective medium theories of Brailsford and Wynblatt (BW) [14] and Marsh and Glicksman (MR) [15] yield the largest coarsening rates as a function of Φ and can be extended to the higher volume fraction region; with the exceptions of Marder (MA) [9] which predicts the largest coarsening rates for $\Phi < 0.05$. The statistical mechanical theories of Marqusee and Ross (MR) [10], and Tokuyama, Kawasaki, and Enomoto (TK) [12] predict lower rate constants. The AK predictions fall mid-range between the statistical mechanical theories of (MR, TK) and effective medium theories (BW, MR) for $\Phi > 0.05$, for $\Phi = 0.05$ AV agrees with BW, and for $\Phi < 0.05$ AV converges to the values of MR and TK. Though the various coarsening theories differ in their prediction of rate constants, there is agreement on the effect of volume fraction on particle size distribution shown in Fig. 6b, the theory of Enomoto, Tokuyama and Kawasaki [13] shows that the steady-state particle size distribution becomes broader and more symmetric than LSW.

In relation to steady-state coarsening experiments in microgravity (ISS), the measured normalized coarsening rate constant ratio (K/K_{LSW}) for $\Phi = 0.3$ is approximately a factor of two times the ratio $(K/K_{LSW})_{AV}$ of AV prediction; the measured value is also higher than predicted by mean field and statistical mechanical theories. However, the microstructure for the 30% volume fraction also shows particle contacts and non-spherical morphology which is outside the theoretical approximations employed in coarsening theories. The particle spatial correlations, given the presence of localized particle distortions due to diffusional interactions with neighboring particles, also did not agree with the AV theory at 30%. The particle size distribution at 30% is slightly wider than theory. For the lowest volume fractions 15% and 20%, the coarsening rate constant and particle size distribution are closer to theory. This appears to show that as the volume fraction decreases better agreement with coarsening theory can be obtained. It remains to address this missing-gap by performing microgravity experiments in the low volume fraction region $\Phi \leq 0.1$ for steady-state condition.

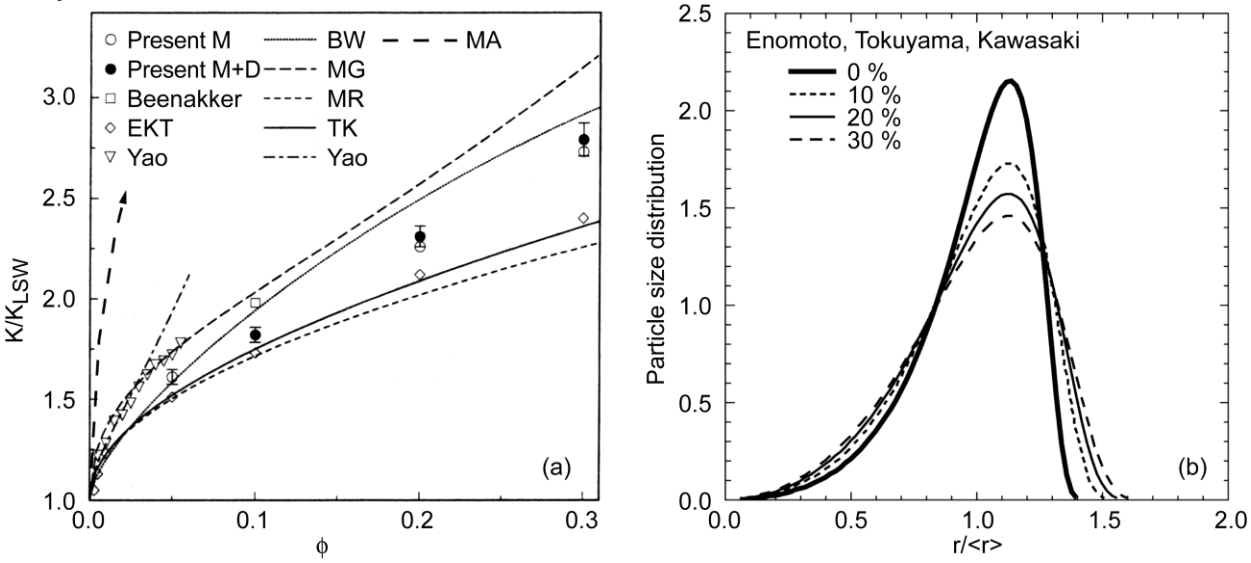

Figure 6. Effect of volume fraction (Φ) on coarsening rate and particle size distribution comparing various theories of Ostwald ripening; (a) prediction of rate constant of the cubic growth rate, K, normalized to the LSW value as a function of volume fraction (Φ) according to: Aikawa and Voorhees (present M and present M+D); Beenaker; Enomoto, Kawasaki, and Tokuyama (EKT); Yao, Elder, Guo and Grant (Yao), Brailsford and Wyndblatt (BW), Marsh and Glicksman (MG), Marqusee and Ross (MR); Tokuyama, Kawasaki and Enomoto (TK), (b) The Enomoto, Tokuyama and Kawasaki theory for predicting steady-state particle size distribution at various volume fractions.

Concluding Remarks

The microgravity environment (Shuttle/ISS) facilitates the performance of coarsening experiments through elimination of sedimentation and buoyancy-induced convection effects. Analysis of the quenching phase, through computational solution of a transient two-dimensional model of the dynamical equations of motion, show that the Peclet number is much less than one and the particle displacement is much less than the average particle size. This implies that coarsening was diffusion limited and the spatial distribution of particles on ISS/Shuttle were not

affected by quenching. The low volume fraction $\Phi = 0.1$ coarsening experiment performed on the Shuttle (CSLM-1) showed clear evidence of transient coarsening. The experiments performed on ISS (CSLM-2) for $\Phi \geq 0.15$ achieved steady-state condition; there was no evidence of transient coarsening. The coarsening rate for the 30% volume fraction is higher than predicted by theory with a particle size distribution which is slightly wider than theory. Particle spatial correlations are not that predicted by theory which is in agreement with the observation that even in microgravity the particles are interconnected at 30% volume fraction. However, for the lower volume fraction of 15% the particle size distribution and rate constant are close to theory. The low volume fraction region $\Phi \leq 0.1$ is promising for differentiation between various coarsening theories and presents a challenge for the attainment of steady-state condition in microgravity experiments.

Acknowledgments- We acknowledge D.G. Hall, and C.A. Frey of Zin Technologies for engineering support. Financial assistance is provided by the microgravity program under grant NNX10AV36G through F.P. Chiaramonte. We thank the management at NASA Glenn, J.M. Hickman, F.J. Kohl and T. H. St.Onge for their support.

References

[1] P.W. Voorhees, "The Theory of Ostwald Ripening", *J. of Stat. Phys*., 38(1/1) (1985) 231-252.
[2] P.W. Voorhees, "Ostwald Ripening of Two-Phase Mixtures", Annu. *Rev. Mater. Sci*., 22(1992) 197-215.
[3] I.M. Lifshitz, V.V. Slyozov, "The kinetics of Precipitation from Supersaturated Solid Solutions", *J. Phys. Chem. Solids*, 19 (1961) 35-50.
[4] C. Wagner, "Theorie der Alterung von Niederschlagen durch Umlisen", *Z. Electrochem.*, 65 (1961) 581-591.
[5] P.W. Voorhees, M.E. Glicksman, "Solution to the Multi-Particle Diffusion Problem with Applications to Ostwald Ripening – I. Theory", *Acta metal.* 32(11) (1984) 2000-2111.
[6] P.W. Voorhees, M.E. Glicksman, "Solution to the Multi-Particle Diffusion Problem with Applications to Ostwald Ripening – II. Computer Simulations", *Acta metal.* 32(11) (1984) 2013-2030.
[7] Y. Enomoto, K. Kawasaki, and M. Tokuyama, "Computer Modelling of Ostwald Ripening", *Acta metall.* 35 (1987) 907-913.
[8] C.W.J. Beenaker, "Numerical Simulation of Diffusion Controlled Droplet Growth: Dynamical Correlation Effects", *Phys. Rev. A*, 33(6) (1986) 4482-4485.
[9] M. Marder, "Correlations and Ostwald Ripening", *Phys. Rev. A* 36(2) (1987) 858-874.
[10] J.A. Marqusee and J. Ross, "Kinetics of Phase Transitions", *J. of Chem. Phys.* 79(1) (1983) 373-378.
[11] M. Tokuyama and K. Kawasaki, "Statistical-Mechanical Theory of Coarsening of Spherical Droplets", *Physica A*, 123 (1984) 386-411.
[12] M. Tokuyama, K. Kawasaki, and Y. Enomoto, "Kinetic Equations for Ostwald Ripening", *Physica*, 134A (1986) 323-338.
[13] Y. Enomoto, M. Tokuyama, and K. Kawasaki, "Finite Volume Fraction Effects on Ostwald Ripening", *Acta metal*., 34(11) (1986) 2119-2128.
[14] A.D. Brailsford and P. Wyndblatt, "The Dependence of Ostwald Ripening Kinetics on Particle Volume Fraction", *Acta, Metall.* 27 (1979) 489-497.
[15] S.P. Marsh and M.E. Glicksman, "Kinetics of Phase Coarsening in Dense Systems", *Acta mater*., 44(9) (1996) 3761-3771.
[16] N. Akaiwa and P. Voorhees, "Late-Stage Seperation: Dynamics, Spatial Correlations, and Structure Functions", *Phys. Rev. E*, 49(5) (1994) 581-591.
[17] M.K. Chen and P.W. Voorhees, "The Dynamics of Transient Ostwald Ripening", *Model. Sim. In Mat. Sci. and Eng.*, 1(1993) 591-612.
[18] J.H. Yao, K.R. Elder, H. Guo, M. Grant, "Theory and Simulation of Ostwald Ripening", *Phys. Rev. B*, 47(21) (1993) 14110-14124.
[19] S.C. Hardy, G.B.McFadden, S.R. Coriell, P.W. Voorhees, R.F. Sekerka, "Measurement and analysis of Grain Boundary Grooving by Volume Fraction", *J. Cryst. Growth*, 114 (1991) 467-480.
[20] W.M.B. Duval, "Flow Field Topology of Transient Mixing Driven By Buoyancy", *Chaos*, 14(3) (2004) 716-738.
[21] W.M.B. Duval, D.J. Chato, M.P. Doherty, "Transient Convection Due to Imposed Heat Flux: Application to Liquid Acquisition Devices", *AIAA* 2011-1321.
[22] E.B. Gulsoy, K. Wittman, J. Thompson, and P.W. Voorhees, "Coarsening in Solid-Liquid Mixtures: Effect of Microgravity Accelerations on Particle Sedimentation", *AIAA* 2011-1346.
[23] L. Ratke, P.W. Voorhees, *Growth and Coarsening: Ripening in Materials Processing* (Springer-Verlag, Germany, 2002) 43-55, 167-203.
[24] J. Alkemper, V Snyder, N. Akaiwa, and P. W. Voorhees, "The Dynamics of Late Stage Phase Seperation: A Test of Theory", *Phys. Rev. Lett.* 82(13) (1999) 2725-2728.
[25] V.A. Snyder, J. Alkemper, and P.W. Voorhees, "The Development of Spatial Correlations during Ostwald Ripening: A Test of Theory", *Acta Materiala*, 48(10) (2000) 2341-2348.
[26] D.J. Rowenhorst, J.P.Kuang, K. Thorton, P.W. Voorhees, "Three-Dimensional Analysis of Particle Coarsening in High Volume Fraction Solid-Liquid Mixture", *Acta Materiala* 54 (2006) 2027-2039.
[27] D.Kammer, A. Geneau, P.W.Voorhees, W.M. Duval, R.W. Hawersaat, J.M. Hickman, T.Lorik, D.G. Hall, C.A.Frey, " Results from the International Space Station: Coarsening in Solid-Liquid Mixtures", *AIAA* 2009-616.
[28] J.R. Thomson, J. Casademunt, F. Drolet, J. Vinals, "Coarsening of Solid-Liquid Mixtures in a Random Acceleration Field", *Phys. Fluids*, 9(5) (1997) 1336-1343.